Changes in gene expression during female reproductive development in a color polymorphic insect

Beatriz Willink,[1,2] (iD) Mary Catherine Duryea,[3] Christopher Wheat,[4] and Erik I. Svensson[1,5] (iD)

[1]*Department of Biology, Evolutionary Ecology Unit, Ecology Building, Lund University, Lund 223–62, Sweden*

[2]*Current Address: School of Biology, University of Costa Rica, San José 11501–2060, Costa Rica*

[3]*Science Department, Southern New Hampshire University, Manchester, New Hampshire 03106*

[4]*Department of Zoology, Stockholm University, Stockholm S-106 91, Sweden*

[5]*E-mail: erik.svensson@biol.lu.se*

Pleiotropy (multiple phenotypic effects of single genes) and epistasis (gene interaction) have key roles in the development of complex phenotypes, especially in polymorphic taxa. The development of discrete and heritable phenotypic polymorphisms often emerges from major-effect genes that interact with other loci and have pleiotropic effects on multiple traits. We quantified gene expression changes during ontogenetic color development in a polymorphic insect (damselfly: *Ischnura elegans*), with three heritable female morphs, one being a male mimic. This female color polymorphism is maintained by male mating harassment and sexual conflict. Using transcriptome sequencing and de novo assembly, we demonstrate that all three morphs downregulate gene expression during early color development. The morphs become increasingly differentiated during sexual maturation and when developing adult coloration. These different ontogenetic trajectories arise because the male-mimic shows accelerated (heterochronic) development, compared to the other female morphs. Many loci with regulatory functions in reproductive development are differentially regulated in the male-mimic, including upstream and downstream regulators of ecdysone signaling and transcription factors potentially influencing sexual differentiation. Our results suggest that long-term sexual conflict does not only maintain this polymorphism, but has also modulated the evolution of gene expression profiles during color development of these sympatric female morphs.

KEY WORDS: Ecdysone, epistasis, heterochrony, pleiotropy, regulatory network, sexual dimorphism.

The role of epistasis (gene interaction) in shaping phenotypic variation and covariation has been discussed since the early days of the Modern Synthesis (Fisher 1930; Wright 1930; 1931), and still remains a contentious subject (Hill et al. 2008; Shao et al. 2008; Huang et al. 2012; Hemani et al. 2014; Mackay 2014; Wood et al. 2014). Epistasis occurs when the phenotypic effect of a gene or genetic variant depends on the genotype of other loci. Major-effect loci affect multiple traits by operating on top of gene regulatory networks (Tyler et al. 2009). Allelic variants in major-effect loci can therefore cause extensive phenotypic differentiation by interacting epistatically with downstream genes in modular regulatory networks (Monteiro and Podlaha 2009).

Color-polymorphic taxa provide interesting model systems for investigating the epistatic interactions by which master-regulatory loci cause pronounced phenotypic differentiation. Heritable color morphs typically differ in multiple physiological, developmental, and life history traits (McKinnon and Pierotti 2010). Yet, color polymorphisms often have a relatively simple genetic basis of one or a few loci with restricted recombination in between them (Joron et al. 2006; Lamichhaney et al. 2016; Lindtke et al. 2017; Andrade et al. 2019). The genetic basis and molecular mechanisms behind the phenotypic differences of such heritable color morphs can therefore reveal direct or indirect interactions between color-morph loci and other loci influencing

suites of phenotypic traits. Although such widespread pleiotropic effects of color-morph loci are increasingly being recognized (Gangoso et al. 2016; Dijkstra et al. 2017; Toomey et al. 2018; Woronik et al. 2019), we know little about the gene-regulatory effects of color-morph loci, during the critical developmental periods when extensive phenotypic differences between morphs typically emerge.

Phenotypic evolution in animals has many times resulted from regulatory changes in the timing, location, and volume of interactions among gene products (Gerhart and Kirschner 2007). Many evolutionary novelties have arisen through a shift in the relative timing or rate of gene expression (e.g., Gomez et al. 2008; Albertson et al. 2010; Gunter et al. 2014), rather than due to the disruption of previous interactions or through the formation of entirely novel networks. This phenomenon, known as heterochrony was historically considered to be a source of novel phenotypic variation between independently evolving lineages (Gould 1977). However, variation in the timing of developmental events can also be important at the intraspecific level (Linksvayer and Wade 2005). Heterochrony can produce large phenotypic change with only small genetic change (West-Eberhard 2003). Heterochrony may therefore contribute to pervasive phenotypic differences between intraspecific color morphs, if genetic variation in the morph-determining locus controls the timing or relative order of developmental events within morphs.

A small but increasing body of evidence from several color polymorphic taxa suggests that genetic control over regulatory networks can produce substantial intraspecific phenotypic variation (Kunte et al. 2014; Timmermans et al. 2014; Yassin et al. 2016; Takahashi et al. 2018). Such gene regulatory networks may modify both the identity of interacting genes and the relative timing of conserved interactions (e.g., Pham et al. 2017). Developmental characterization of gene expression profiles of color polymorphic taxa is a first step to assess how variation in regulatory targets and in the timing of regulatory events causes extensive phenotypic differences between morphs. By investigating direct or indirect interactions between color-morph loci and other loci during development, we can increase our understanding of how epistasis and pleiotropy shape different morphs within species.

Discrete sympatric morphs can emerge as an evolutionary outcome of sexual conflict over mating (Gavrilets and Waxman 2002). For instance, in several insect taxa, female-limited phenotypic polymorphisms have evolved, and their maintenance has been linked to sexual conflict over mating (Svensson et al. 2005; 2009; Reinhardt et al. 2007; Karlsson et al. 2013; Iversen et al. 2019). More recently, such female-limited polymorphisms have also been described in a few vertebrate species, and appear to be promoted by male mating harassment and sexual conflict (Lee et al. 2019; Moon and Kamath 2019). Here, we investigated how changes in gene expression during adult development (i.e., after the last molt) differ among heritable female morphs in the trimorphic common bluetail damselfly (*Ischnura elegans*). Several damselfly species in this genus, including *I. elegans*, express such female-limited color polymorphisms that are maintained by frequency-dependent sexual conflict, and in which common morphs suffer from reduced fitness due to excessive male mating harassment (Svensson et al. 2005; Gosden and Svensson 2009; Takahashi et al. 2010; Le Rouzic et al. 2015, Gering 2017).

Two of the female morphs in *I. elegans* differ phenotypically from males in their sexually mature coloration, whereas the third morph is considered to be a male-mimic, with a color pattern strikingly similar to that of males (Svensson et al. 2009). Male-mimicking females also differ from the other two morphs in their ontogenetic trajectories of color change and in several other phenotypic traits, including fecundity (Svensson and Abbott 2005; Willink et al. 2019), mating rates (Gosden and Svensson 2009), parasite resistance and tolerance (Willink and Svensson 2017), cold tolerance (Lancaster et al. 2017), and adult development times (Svensson et al. 2020). Some of these phenotypic differences between the morphs are likely to be adaptive and a result of correlational selection (Svensson 2017). Proximately, morph differences may arise because the color locus (or a set of tightly linked loci) directly or indirectly regulates other loci affecting co-selected traits. Such regulatory interactions can be investigated by comparing gene expression profiles during ontogenetic development of the female morphs. Quantitative gene expression studies of polymorphic taxa are therefore useful study systems for biologists who are interested in the evolution of gene regulatory networks, and how they are influenced by sexual conflict and sexually antagonistic selection (Hill et al. 2019).

We compared gene expression profiles during ontogeny and color development of the three female morphs in *I. elegans*. The transcriptional differences that we describe and quantify in this study reveal pleiotropic effects of the color locus and illustrate the evolutionary outcome of the long-term sexual conflict and the resulting frequency-dependent selection that has shaped this female polymorphism. Specifically, we compare gene expression profiles of the male-mimicking female morph and the two female morphs that are distinctly different from males in their sexually mature color patterns (Fig. 1A). We address several specific questions about the developmental regulation of gene expression during color development and how it differs between female morphs. First, at which point(s) in color development do female morphs diverge in their gene expression profiles? Second, which physiological processes characterize color development across the female morphs of *I. elegans?* Third, which regulatory genes could cause these differences between the morphs? Finally, are differences in fecundity between morphs due to heterochrony of sexual maturation with respect to color development?
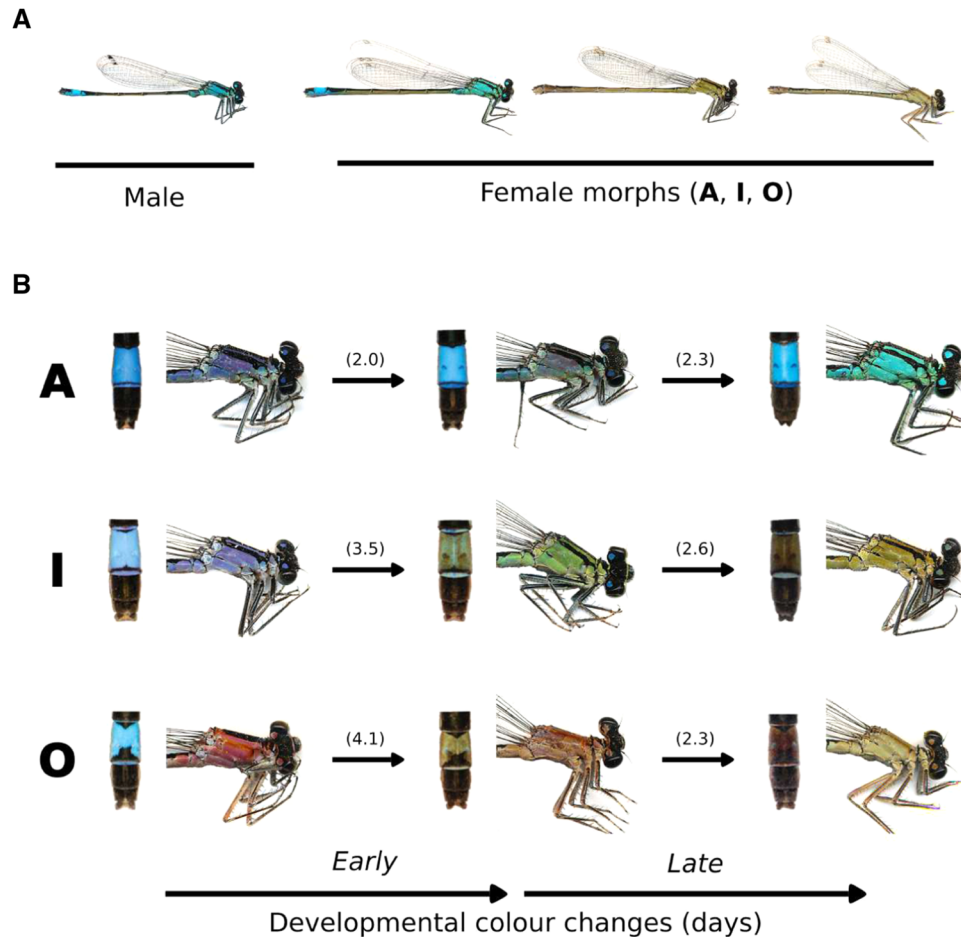
Figure 1. Heritable color polymorphism and ontogenetic color changes in females of the common bluetail damselfly (*Ischnura elegans*). (A) Male and the three female-limited color morphs of *I. elegans* in their final, sexually mature developmental phase. The color pattern of sexually mature A-females is remarkably similar to that of males, and hence they are considered to be male mimics. (B) Ontogenetic color changes in the distal abdomen segments (left) and the thorax (right) of females of the three color morphs in *I. elegans*. The columns correspond to females in the *immature*, *transitional*, and *mature* developmental color phases. The rows represent color changes within each heritable morph. The numbers in parenthesis give the mean number of days for each color transition, when females were kept in large outdoor mesocosm enclosures from their immature phase until sexual maturity (see Fig. S1).

Apart from gaining a better understanding of the molecular mechanisms underlying the female color polymorphism in *I. elegans* and other polymorphic damselflies, the answers to the questions above should also be of general interest for the genomic consequences and evolutionary outcomes of various forms of sexual conflict (Rowe et al. 2018). With a few recent notable exceptions (Barson et al. 2015; Cheng and Kirkpatrick 2016; Dutoit et al. 2018), our current empirical knowledge about the genomic signature and consequences of sexual conflict is extremely limited (Rowe et al. 2018). The results in the present study suggest that not only can sexual conflict maintain sexually selected polymorphisms through balancing selection, but such conflict can also shape patterns of pleiotropy, epistasis, gene expression profiles, and gene regulatory networks associated with such polymorphisms (cf. Hill et al. 2019).

Methods

STUDY SYSTEM

Females of the common bluetail damselfly (*Ischnura elegans*) occur in three heritable color morphs, whereas males are monomorphic (Fig. 1A). Female morphs differ in both their sexually mature (final) color patterns as well as in the qualitative color changes that are expressed during sexual development (Cordero et al. 1998; Svensson et al. 2009; Willink et al. 2019; Fig. 1). Previous studies using breeding experiments in controlled laboratory environments across multiple generations have revealed that color morph development is governed by a single autosomal locus (or a set of tightly linked loci) with sex-limited expression to females (Cordero 1990; Sánchez-Guillén et al. 2005). In *I. elegans*, these female morphs are typically referred to as "Androchrome," "Infuscans," and "Infuscans-obsoleta." To

be consistent with previous publications (Willink and Svensson 2017; Willink et al. 2019), we hereafter refer to these three heritable female morphs as A-, I-, and O- females.

Shortly after emergence from their last nymphal molt, A- and I-females exhibit a thoracic violet background color with black antehumeral stripes (Fig. 1B). In A-females, the violet color becomes turquoise-blue over postemergence development, and therefore the final thoracic color pattern of sexually mature A-females strikingly resembles the color of males (Fig. 1). This adaptive color change in A-females is consistent with male mimicry, by which A-females avoid excessive and costly male-mating harassment (Gosden and Svensson 2009; Gering 2017). In contrast, the violet thorax color of I-females becomes greenish-brown in association with increased reproductive output (Willink et al. 2019; Fig. 1B). Finally, O-females are also distinct from males when sexually mature, but they do not exhibit ante-humeral stripes at any point in development and their thoracic color changes from salmon-pink to brown (Cordero et al. 1998; Willink et al. 2019; Fig. 1B).

The two nonmimicking morphs, I- and O-females, exhibit dramatic ontogenetic changes in the phenotypic expression of a blue patch on the eighth abdominal segment (Fig. 1B). This blue abdominal patch is initially present in sexually immature individuals of all three female morphs (Fig. 1B). However, in I- and O-females the blue patch subsequently becomes concealed by dark pigment over sexual development, whereas in males and the male-mimicking A-females, the blue coloration is instead retained during the entire course of sexual development (Henze et al. 2019; Fig. 1). All three female morphs therefore undergo ontogenetic color changes over sexual development, but there are pronounced differences between A-females and the two other female morphs (I- and O-females). These color changes occur continuously over the span of a few days (Svensson et al. 2020; Figs. 1B and S1). During this transitional period, individual females with intermediate phenotypes between the immature and mature developmental phases can be visually distinguished (Fig. 1B).

FIELDWORK AND SAMPLING DESIGN

We sampled three females of each heritable color morph at three stages of color development, using the detailed description and classification of these color stages by Cordero et al. (1998) and Svensson et al. (2009). The *immature* developmental phase was defined in all morphs by the presence of a contrasting blue color patch in the distal portion of the abdomen, and for A-females by the simultaneous expression of the violet thoracic coloration. Females were classified to the *mature* developmental phase if they expressed the final color phenotype of sexually mature in-dividuals of their respective morph. Finally, *transitional* females expressed an intermediate phenotype between these two ex-

tremes. For I- and O-females, these *transitional* individuals were identified by partial concealment of the blue patch with pigment, which results in a brownish-blue abdominal patch (Fig. 1B). *Transitional* A-females were characterized by a violet-turquoise thoracic coloration, which precedes the development of the final turquoise-blue background color (Fig. 1B). All individuals in this study were collected in the field in southern Sweden during the summer (12 June to 7 July) of 2015. All individuals were col-lected during morning hours and from populations that form part of a long-term longitudinal study, in an area of approximately $40 \times 40 \text{ km}^2$ (Table S1; Svensson et al. 2005; Le Rouzic et al. 2015; Willink and Svensson 2017).

RNA SAMPLE PREPARATION AND SEQUENCING

In addition to the 27 females sampled for the differential gene expression (DGE) analysis, 56 *mature*-colored females were sampled and used for the de novo transcriptome assembly below (Table S1). Field-caught individuals were bisected at the second abdominal segment and the two sections were preserved in RNAlater immediately following bisection, and stored at –80°C within 1–4 h of capture. Samples were then shipped to the Beijing Genomics Institute (1/F, 16th Dai Fu Street, Tai Po Industrial Estate, Tai Po, Hong Kong) for extraction and sequenc-ing. Total RNA was extracted from whole bodies using the Trizol LS Reagent (Life Technologies) following the manufacturer's instructions. RNAseq libraries were prepared for individual sam-ples using the Illumina TruSeq kit with mRNA enrichment. Each sample was sequenced using 100 bp paired-end reads at a depth of 2 GB per sample on an Illumina HiSeq 2000. Raw data were deposited at the National Center for Biotechnology Information (NCBI) Sequence Read Archive (BioProject #PRJNA624641).

TRANSCRIPTOME ASSEMBLY AND ANNOTATION

Raw reads were trimmed using Trimmomatic version 0.36 (Bolger et al. 2014) to remove adapter sequences and ambiguous nucleotides. We cropped the first 10 nucleotides of each read and trimmed regions of four nucleotides that had an average quality score below 20. Reads shorter than 25 nucleotides after trimming were discarded. The number of reads per sample after trimming was $9,982,724 \pm 1,052,611$ (mean $\pm$ SD), for all samples used in the DGE analysis. Trimmed reads from all 83 samples were pooled to assemble a reference transcriptome using Trinity version 2.2.0 (Grabherr et al. 2011). This is the recommended approach for RNAseq analyses on novel species to include more of the alternative splice isoforms in the final reference for mapping (Haas et al. 2013).

Assembly quality was assessed by generating Ex50 esti-mates using scripts from the Trinity package (Haas et al. 2013), and by quantifying the ortholog hit ratio (OHR) (Vera et al. 2008; O'Neil et al. 2010; O'Neil and Emrich 2013). Ex50

estimates were generated by plotting the N50 of contigs for different expression quantiles, searching for the maximal N50 for regions capturing 70–90% of the expression data. OHR estimates were generated using the predicted protein set from the genome of the banded demoiselle damselfly, *Calopteryx splendens* (Csple_OGS_v1.0.faa; Ioannidis et al. 2017), then using blast (tblastn; Camacho et al. 2009) to search for the best hit of each protein in the *I. elegans* transcriptome assembly. OHR was then estimated by dividing the aligned length of an *I. elegans* transcript contig by the length of its orthologous *C. splendens* protein, wherein ratios of 1 indicate the full coverage of the contig for a given protein. The result was a single OHR estimate for each nonredundant protein from a related damselfly, the ortholog of which was found in the *I. elegans* transcriptome. The OHR distribution provides a detailed assessment of a transcriptome, indicating how well thousands of genes have been assembled. Prior to analysis, redundancy due to isoforms and duplications in the *C. splendens* protein set was controlled by collapsing it by the longest protein isoform of each protein cluster group. This was based upon >90% amino acid identity using CD-HIT version 4.5.4 (Li and Godzik 2006) with parameters used in making the UniRef90 database (Suzek et al. 2014).

Annotation of the reference transcriptome was conducted using *blastx* version 2.6.0+ with an e-value of 10×10^{-5} against the NCBI nonredundant database (nr). Blast hits were then mapped to Gene Ontology (GO) terms using Blast2GO version 4.1.9 (Conesa et al. 2005). If the blasted sequences returned more than a single hit, only the highest scoring hit was used in subsequent GO enrichment analysis.

DATA PREPROCESSING

Prior to the DGE analysis, we used the CORSET algorithm (Davidson and Oshlack 2014) to reduce the number of spurious isoforms, which often arise during de novo transcriptome assemblies of nonmodel organisms due to sequencing artefacts. CORSET hierarchically clusters contigs based on shared reads and expression levels. In this case, clusters were based on the 27 samples to be used in our DGE analysis. The read counts are then summarized by these clusters, providing gene-level transcript abundances. Lowly expressed genes (i.e., with fewer than one read per million reads in at least three samples) were discarded at this stage and gene expression distributions were normalized via the weighted trimmed mean of M-values (TMM) method (Robinson and Oshlack 2010).

DGE ANALYSIS

DGE analyses were conducted using the packages *edgeR* (Robinson et al. 2010; McCarthy et al. 2012) and *limma* (Ritchie et al. 2015) in R version 3.6.3 (R Core Team 2020) and were based on the workflow described by Law et al. (2016). To apply linear-based statistical modeling to the expression data, we estimated the mean-variance relationship in the log transcript counts per million (log-cpm), and incorporated this mean-variance trend into a precision weight for each normalized observation, using the voom method (Law et al. 2014; Liu et al. 2015). The advantage of this statistical approach, which estimates the mean-variance relationship instead of specifying a generating probabilistic distribution, is that it more appropriately controls for type I error rates when sample sizes are small and when sequencing depth varies between samples (Law et al. 2014; Liu et al. 2015). In the *limma* pipeline, these precision weights are then taken into account when fitting the linear models to the log-cpm gene expression data (Law et al. 2016). Empirical Bayes moderation was subsequently applied to these fitted models to more accurately estimate expression variability among genes and the "robust" procedure was employed to allow variance outliers (Smyth 2004; Law et al. 2014; Phipson et al. 2016). Multiple testing across statistical contrasts was conducted using the "global" method, which is recommended when the number of differentially expressed (DE) genes is interpreted as a measure of the strength of a contrast (Smyth et al. 2018). The "global" method performs multiple testing adjustment across the entire set of contrasts and genes being tested. The *P*-value cutoff was adjusted according to Benjamini and Hochberg's false discovery rate (Benjamini and Hochberg 1995).

Our goal was to compare DGE across developmental stages and between the different color morphs. Thus, we fitted a fully factorial linear model including the fixed effects of female color morphs, developmental color phases, and their interaction (∼0 + Morph + Phase + Morph:Phase). With this model structure, the intercept is removed from the first factor (Morph), but kept in the second factor (Phase). Therefore, within each morph the immature phase is the intercept, and expression differences between groups can be compared by specifying a contrast matrix. Three types of comparisons (hereafter contrast groups) are possible with the interaction term: (1) contrasts among morphs within each color development phase, (2) contrasts between subsequent phases within morphs, and (3) contrasts among color morphs with regard to the direction and magnitude of gene expression changes across development (full contrast matrix in Table S2). Because we sampled three females of each of three morphs and at each of three phases in color development (27 females in total), developmental comparisons in contrast groups (2) and (3) span one of two windows of color development: *early* color development, between the *immature* and *transitional* phases, and *late* color development, between the *transitional* and *mature* phases (Fig. 1B). Our main focus in this study was on contrast group (3), because these contrasts represent changes in expression between developmental color phases that are opposite in direction or different in magnitude between morphs. We used contrast group (2) to identify genes that are differentially

expressed during the course of color development within morphs. We also used contrasts in (2) to identify the biological processes that are enriched during color transitions for each female morph. These analyses are summarized in the next two sections. The results of contrasts among morphs within each phase (1) are presented in the Supporting Information (Fig. S2).

The ontogenetic color changes are not of equal duration in all three morphs (Svensson et al. 2020). I- and O-females take a longer time to complete their color maturation, compared to A-females (Figs. 1B and S1). As mentioned above, we determined the *transitional* color phase as being visually intermediate between the *immature* and *mature* color phases. The *transitional* color phase is reached approximately at the midpoint of the color development period in A-females (Fig. 1B). In contrast, I- and O-females that appear intermediate in color between the *immature* and *mature* color phases are both older on average than *transitional* A-females, and past the midpoint of their color development period (Fig. 1B). Consequently, I- and O-females have a protracted *early* color development compared to A-females, whereas *late* color development is of a similar duration for all female morphs (Figs. 1B and S1).

CORRELATIONS AMONG SUBSETS OF DIFFERENTIALLY EXPRESSED GENES

We used vector correlations to determine if developmental expression changes shared similar patterns across morphs for each color transition (*early* and *late* color development). Vector correlations are useful to assess the similarity between estimated contrasts of gene expression across a set of multiple genes (Zinna et al. 2018). The correlation between two mean-centered vectors, each containing the estimated magnitude of expression differences between two experimental categories, is as follows:

$$r_{vc} = \frac{|a \cdot b|}{\|a\| \times \|b\|}, \tag{1}$$

where $a \cdot b$ is the dot product between the two vectors of statistical contrasts and $\|a\|$ and $\|b\|$ represent the magnitudes of vectors a and b, respectively, and are given by the square root of the sum of squares of all contrast estimates. The gene vectors a and b in this study correspond to log-transformed coefficients estimated from the linear model and contrast matrix described above (Table S2). The vector correlation r_{vc} is equivalent to the Pearson correlation coefficient, such that values close to 1 indicate an almost perfect correlation between gene expression vectors, values close to 0 indicate no correlation, and values close to -1 indicate nearly opposite regulation of gene expression between the two vectors.

We followed the approach of Zinna et al. (2018) to determine if vector correlations between contrasts that have been considered significantly different from zero were particularly strong, compared to correlations between vectors of a random sample of genes, irrespective of the degree of statistical significance. This would indicate that those genes with significant changes in expression across a period of color development (contrast group [2]; Table S2) are also more similar (or dissimilar) in the direction of their regulation than a random gene vector of equal length. We defined in each case an experimental vector, for example, a vector containing all differentially expressed genes during *early* color development that are shared between two female morphs. We then obtained an empirical distribution of vector correlations, drawn from 10,000 randomly sampled vectors of the same length as the experimental vector. We considered a correlation for the experimental vector as extreme when it fell outside the 95 percentile of correlations in equal-length random vectors.

GO ENRICHMENT ANALYSIS

To uncover the physiological changes that follow color transitions in the different female morphs, we tested for significantly enriched GO terms in groups of developmentally regulated genes (i.e., genes with significant changes in expression between consecutive color phases) in comparison to the reference transcriptome, using the bioconductor package TopGO (Alexa and Rahnenfuhrer 2016) in R. For these analyses, we focused on contrasts between developmental color phases within morphs (contrast group [2]; Table S2). In the cases where multiple transcripts associated with a single gene (i.e., a CORSET cluster) differed by at least one GO term (2231 out of 30,134 mapped transcripts), all GO terms mapped to the different transcripts were pooled, and every unique term was assigned to the gene. Given that our interest was to explore how physiological processes change over development in the three female morphs, here we focused on biological process ontologies. The significance of enriched terms was tested using Fisher's exact test and the "*elim*" algorithm to account for the hierarchical structure of gene ontologies (Alexa et al. 2006). With this algorithm, more general annotations are excluded for genes already counted as significantly enriched for a more specific GO term. GO terms with P-values <0.01 were considered significantly enriched in the gene set of interest, compared to the reference transcriptome.

COLOR DEVELOPMENT, HETEROCHRONY, AND FEMALE FECUNDITY

A-females reach their final developmental color phase at a younger age than I- and O-females (Svensson et al. 2020; Fig. 1B). This suggests that unlike color changes in I- and O-females, color changes in A-females might be decoupled from sexual maturation. If so, previous records of lower fecundity of A-females compared to I-females (Willink et al. 2019) may be owed to the average younger age of mature-colored A-females in the field. To test the idea that color development could be faster

(i.e., heterochronic) than most other developmental changes, including sexual maturation, in A-females, we first compared *early* and *late* expression changes within each female morph, using the vector correlation approach described above. A-females reach their mature color at a similar absolute age as I- and O-females develop their *transitional* phase (Svensson et al. 2020; Fig. 1B). If most other developmental changes proceed at similar rates in all female morphs, we would expect expression contrasts in *early* and *late* color development to be more correlated in A-females than in the other two morphs, as in A-females these two developmental periods span a shorter absolute time. In contrast, if the fast color changes of A-females indicate overall faster development, we would expect *early* and *late* expression contrasts to be as different in A-females as in I- and O-females, despite the shorter duration of *early* color development in A-females.

Furthermore, if A-females accelerate their color maturation in relation to sexual maturation, we expect that mature-color A-females in the field would more often be sexually immature, and exhibit a higher rate of reproductive failure than I- and O-females. Our fecundity data to test this prediction come from our surveys of 18 natural populations in Southern Sweden, which were visited frequently during the mating season (June to August) for 2–17 years, between 2001 and 2017 (Svensson et al. 2005; Le Rouzic et al. 2015; Willink and Svensson 2017). During these visits, mating couples were collected in the field. Mated females were placed in individual plastic containers with moist filter paper for oviposition. After 72 h, eggs were scanned at 1200 dpi and subsequently counted using ImageJ (Schindelin et al. 2012).

In these surveys, mated females were classified by morph and developmental phase. However, *transitional* females were not classified as such, and before 2015 we did not distinguish between A- and I-females in the *immature* developmental phase (Fig. 1B). Therefore, we modeled the probability of reproductive failure only for the *immature* and *mature* developmental phases, and all data on *immature* A- and I-females come from the last three years of our population survey (2015–2017). We used a mixed-effect model fitted by MCMC in the *R* package MCMCglmm (Hadfield 2010) to test for a difference between morphs in the probability of reproductive failure, which we defined here as mated females that produced no viable eggs. We specified a binomial model with morph, developmental phase, and their interaction as fixed effects. We also allowed for a random interaction between the population and season terms to affect the variance around the fixed effect estimates. All code to reproduce these analyses as well as the reproductive failure data are available in Dryad (https://doi.org/10.5061/dryad.g1jwstqnd).

Table 1. Number of differentially expressed (upregulated and downregulated) and similarly expressed (N.S.) genes, in comparisons between developmental color phases and within female color morphs of *I. elegans*. Developmental comparisons are performed between the *immature* and *transitional* phases (*early* color development) and between the *transitional* and *mature* developmental phases (*late* color development). A total of 27 females were sampled for this analysis, three of each color morph in all three developmental phases.

Color transition	Morph	Upregulated	Downregulated	N.S.
Early	A	198	5210	20,972
	I	301	4191	21,888
	O	950	4678	20,752
Late	A	3257	1730	21,393
	I	365	345	25,670
	O	240	475	25,665

Results

REFERENCE TRANSCRIPTOME

Using an extensive collection of RNA-Seq data, we assembled a transcriptome of 889,001 transcripts. Grouping transcripts by their expression levels and looking at those with the highest levels of expression in relation to their assembly lengths, a peak of transcript assembly length (N50) of nearly 3 kb was found at expression levels containing 70–80% of transcripts (i.e., ExN50 ∼3 kb), suggesting sufficient data for a high-quality assembly. We also estimated the OHR of our assembly by querying our assembly with the full protein set of the only published odonate genome, the banded demoiselle damselfly (*Calopteryx splendens*), which shared a common ancestor with *I. elegans* approximately 85 million years ago (the average from two dated phylogenies, 92 million year in Thomas et al. 2013 and 79 million years in Waller and Svensson 2017). Of the 22,507 *C. splendens* proteins that were nonredundant, we found good hits (e-value less than 10×10^{-5}) for roughly 19,962, and of these, we found OHR of 0.7 and higher for nearly 70% (13,497; see Fig. S2 and Table S3). Given the extensive divergence between the two taxa, the number of putative orthologs between species recovered is high and the strong skew toward high OHR values is indicative of a high-quality transcriptome assembly.

### GENERAL TRENDS IN EARLY COLOR DEVELOPMENT

In all female morphs, *early* color development was characterized by an extensive decrease in gene expression between the *immature* and *transitional* phases (contrast group [2]; Table 1; Table S2). Across-the-board downregulation from the *immature* to the *transitional* phase exceeded upregulation by a factor of more than 4, in O-females, to more than 25, in A-females (Table 1).

Of all downregulated genes during *early* color development, 3158 were shared by the three female morphs, whereas there were no upregulated genes shared by all morphs. The downregulated genes shared by all female morphs corresponded to ~60%, 75%, and 67% of all downregulated genes in A-, I-, and O-females, respectively. These genes were significantly enriched for biological processes involved in protein synthesis, transport and catabolism, energy metabolism, signal transduction, and catecholamine biosynthesis (Table S4). Broadly shared downregulation of gene expression across *early* color development also resulted in highly correlated vectors of genes with significant expression changes between all morph pairs (Fig. 2A).

GENERAL TRENDS IN LATE COLOR DEVELOPMENT

No significant expression changes from the *transitional* to the *mature* color phase (contrast group [2]; Table S2) were shared by all female morphs. This absence of shared regulatory patterns during *late* color development was caused by the distinctiveness of A-females. There was a perfect negative correlation between A- and I-females in the regulation of genes that were differentially expressed in both morphs (Fig. 2A). Of 268 genes with significant expression changes between the *transitional* and *mature* color phases, 164 increased in expression in I-females and decreased in expression in A-females, whereas 104 exhibited the opposite regulatory pattern. There was also a negative correlation in the direction of regulation for the genes differentially expressed across *late* color development in A- and O-females, but this correlation was not particularly extreme ($P = 0.21$). Most genes, whether significant or not, exhibited opposite developmental contrasts between A- and O-females during *late* color development. In contrast, there were 65 genes with significant changes in expression across *late* color development in both I- and O-females, and all of these genes were regulated in the same direction in both morphs (i.e., either increased or decreased in expression between the *transitional* and *mature* color phases; Fig. 2A).

The biological processes enriched in DE genes during *late* color development were also markedly different between A-females and both I- and O-females. Compared to the *transitional* color phase, *mature*-color A-females upregulated genes enriched for functions in cell cycle progression, meiosis, and the regulation of transcription, while downregulating multiple processes associated with energy metabolism (Tables S6 and S7). Both I- and O-females in their *mature* color phase upregulated energy metabolic processes compared to their *transitional* color phase (Table S7). *Mature*-color I-females downregulated lipid metabolism and gene silencing and *mature*-color O-females downregulated genes participating in cell cycle progression and protein and RNA modification, compared to females of these morphs in the *transitional* color phase (Table S6).
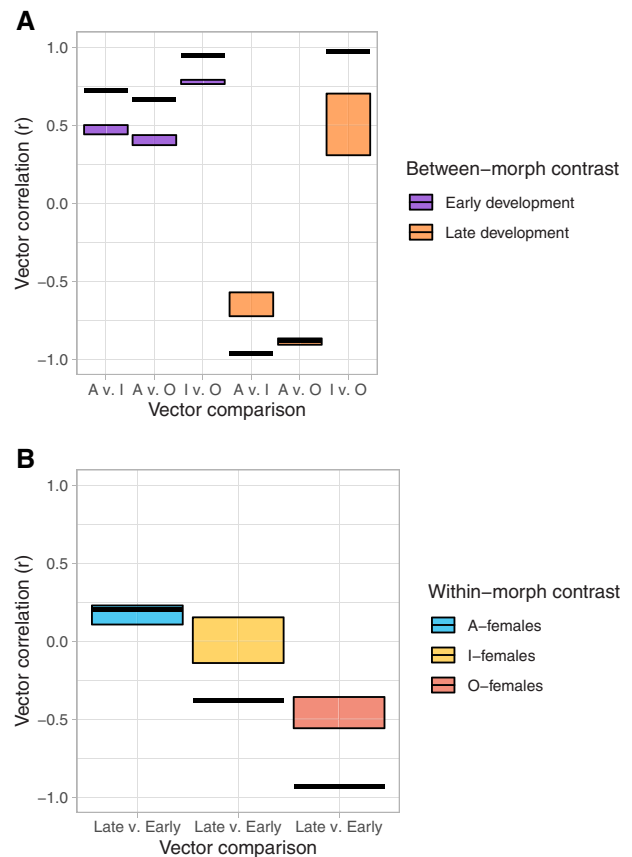

Figure 2. Vector correlations of gene expression contrasts. We tested for overall similarity in the expression changes underlying color development (A) between all female-morph pairwise comparisons during *early* and *late* color development, and (B) between *early* and *late* color development within each female morph. Vector correlations (*r*) indicate the similarity in the direction of change in gene expression between two vectors of developmental contrasts. Values close to 1 suggest that the two vectors are nearly identical in direction, whereas values close to –1 suggest developmental regulation of gene expression is opposite in direction between the two vectors. The black horizontal lines show correlation values for experimental vectors (sets of differentially expressed genes, see Methods); the colored boxes show the 95 percentile of empirical distributions of 10,000 contrast vectors of the same length as the experimental vectors, but including a random sample of all genes. The lengths of the experimental gene vector from left to right are 3531, 3590, 3732, 268, 656, and 65 for (A) and 1054, 181, 223 for (B).

COLOR DEVELOPMENT HETEROCHRONY AND FEMALE FECUNDITY

I- and O-females underwent a qualitative change in the direction of gene regulation between *early* and *late* color development. DE genes that increased in expression between the *immature* and *transitional* color phase (*early* color development) tended to decrease in expression between the *transitional* and *mature* color phase (*late* color development), and *vice versa* (Fig. 2B). In
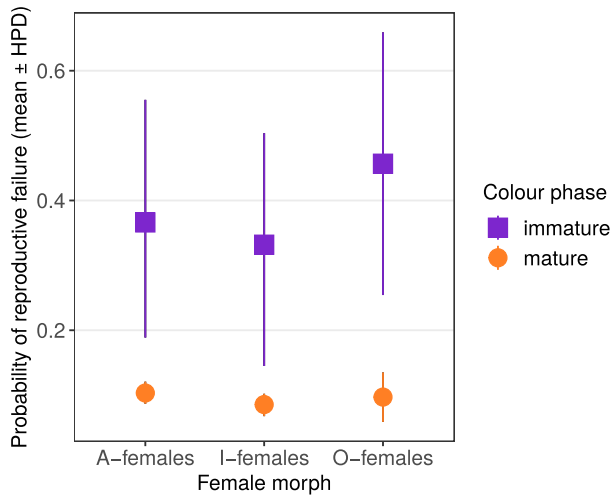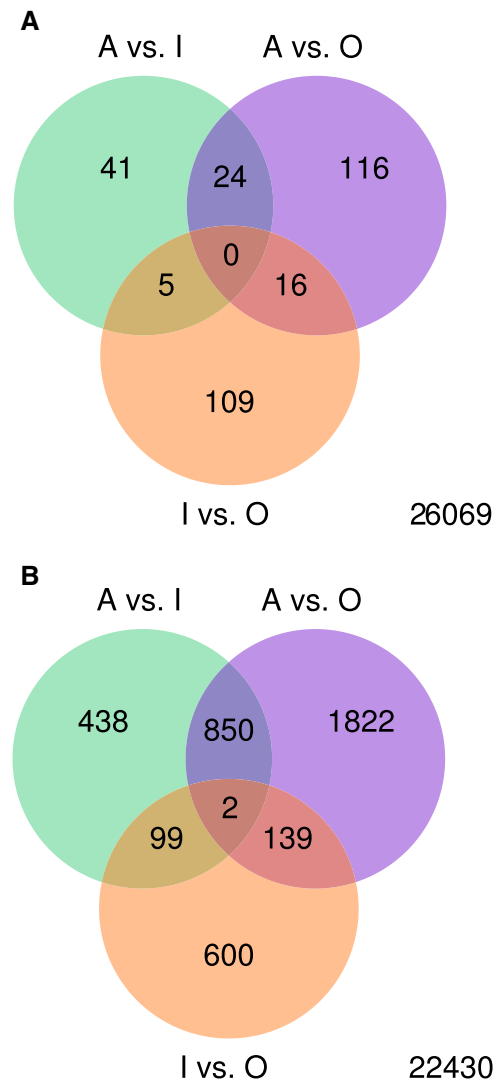
Figure 3. Probability of reproductive failure, quantified as the proportion of mated females laying no viable eggs, among three female morphs and two developmental color phases of *I. elegans*. The symbols show the posterior mean and 95% highest posterior density (HPD) intervals of parameter estimates in a binomial mixed-effect model fitted by MCMC.


Figure 4. Venn diagram showing the genes that were differentially regulated across color development, between pairs of female morphs of *I. elegans* (i.e., genes with significant differences between morphs in the direction or magnitude of developmental changes; contrast group [3]; Table S2). **(A)** *early* color development, **(b)** *late* color development. The number of genes with no evidence of morph differences in differential expression between developmental color phases is shown in the bottom right corner of each plot.

contrast, regulation of gene expression was positively, although not extremely, correlated between *early* and *late* color development in A-females (Fig. 2B). Such positive correlation between developmental periods in A-females was not extreme when compared to a random sample of expression contrasts drawn from equal-length gene vectors regardless of their significance level ($P = 0.175$; Fig. 2B). Nonetheless, DE genes that decreased in expression through both *early* and *late* color development in A-females were enriched for two shared biological processes, both associated with ATP biosynthesis (Tables S4 and S6). DE genes across *early* and *late* color development did not share any enriched biological processes for either I- or O-females.

We obtained data on reproductive failure of 5247 (sample sizes for A-, I-, and O- females: $N_A = 3\,36$, $N_I = 1667$, $N_O = 234$) *mature*-color and 93 ($N_A = 28$, $N_I = 34$, $N_O = 21$) *immature*-color females, all mated in the field. Across these three female morphs, *immature* developmental phases exhibited a nearly fourfold probability of reproductive failure compared to their *mature*-color counterparts (posterior probability of *immature*-color females having lower reproductive failure (PMCMC) < 0.001; Fig. 3). There were no differences in the rate of reproductive failure among the three female morphs in the *immature* phase (all PMCMC > 0.05; Fig. 3A). Among *mature*-color individuals, reproductive failure was somewhat higher in A-females compared to I-females (PMCMC = 0.019; Fig. 3B), yet this difference was small relative to differences between *mature*- and *immature*-colored females (Fig. 3).

REGULATORY DIFFERENTIATION DURING COLOR DEVELOPMENT

We tested whether changes in gene expression between consecutive developmental color phases (i.e., developmental regulation) differed in direction or magnitude between female morphs (contrast group [3]; Table S2). There were more substantial morph differences in developmental regulation of gene expression during the second phase of color development (*late* color development; Fig. 4). During this period, A-females were differentiated

Table 2. Ecdysone metabolism genes with different changes in gene expression between A- and both I- and O-female morphs in *I. elegans*, during *late* color development. CORSET clusters are assumed to represent *I. elegans* genes. Transcript sequences in these clusters were blasted against annotated proteins in the *Drosophila melanogaster* (Dmel) genome. For each of the queried *I. elegans* sequences, we report the best Dmel hit, its corresponding gene name, and inferred function.

Cluster ID	Best Dmel hit	Gene name	e-value	Function	References
19875.0	Cytochrome P450 307a1	*spo*	2.73×10^{-9}	Component or positive regulator of ecdysone biosynthesis in the ovary	Ono et al. (2006)
19875.1	Cytochrome P450 307a1	*spo*	4.64×10^{-112}	Component or positive regulator of ecdysone biosynthesis in the ovary	Ono et al. (2006)
24196.1	Ecdysone 20-monooxygenase/ Cytochrome P450 314a1	*shd*	9.93×10^{-103}	Hydroxylates ecdysone to produce 20-hydroxyecdysone (20E)	Petryk et al. (2003)
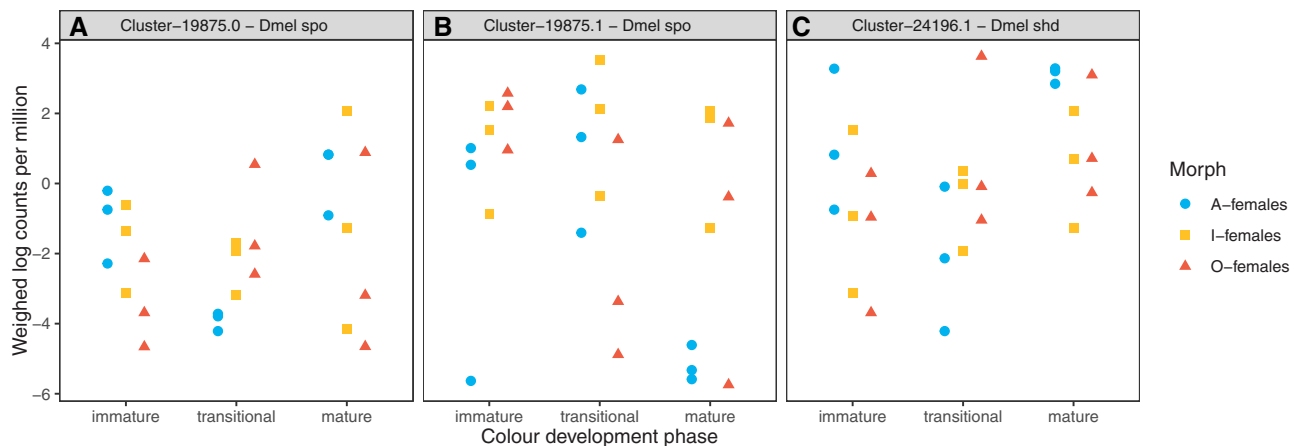
Figure 5. Expression patterns of ecdysone metabolism genes with different changes in gene expression between A- and both I- and O-females during *late* color development of *I. elegans*. Expression data (log counts per million) have been weighed by within-sample variability and by the mean-variance relationship among genes, using "voom" (see Methods). Best hits in the *D. melanogaster* (Dmel) genome are shown in Table 2.

from both I- and O-females in the pattern of developmental regulation of 852 genes (Fig. 4). Statistical contrasts for all these genes were of the same direction between A- and I-females and between A- and O-females.

To examine how epistatic effects of the color-morph locus could mediate the differentiation of A-females, we queried subsets of developmentally regulated genes for regulatory functions. Here, we focused on genes for which the direction or magnitude of developmental regulation differed significantly between A-female and both I- and O-females (contrast group [3]; Table S2). First, we used the search term "juvenile hormone" (JH) and "ecdysone" (E), two major hormones involved in regulating insect reproduction and development (Simonet et al. 2004; Flatt et al. 2005). Although we found no differentially regulated genes directly involved in JH metabolism, four genes related to ecdysone metabolism and signaling exhibited a different developmental change in expression in A-females compared to I- and O-females, during *late* color devel-

opment. None of these genes, or any other ecdysone-related gene, differed in developmental regulation between I- and O-females during *late* color development, and neither did they differ between any pair of morphs during *early* color development. To discern the potential functions of these genes, we used *blastx* against annotated proteins in the *Drosophila melanogaster* genome in FlyBase (Thurmond et al. 2019). Three of these ecdysone-related genes were annotated to *D. melanogaster* genes in the *Halloween* group, which code for Cytochrome P450 enzymes that participate in ecdysone biosynthesis (Table 2; Fig. 5). The fourth gene was annotated as coding for the ecdysone-induced protein E74, a transcription factor that responds to concentrations of 20-hydroxyecdysone (20E) in the ovary of *D. melanogaster* (Table 3; Fig. 6; Ables and Drummond-Barbosa 2010).

We further identified all genes annotated with the GO term "regulation of transcription," within the gene set that underwent unique developmental changes in expression in A-females during *late* color development (Fig. 4B). This query
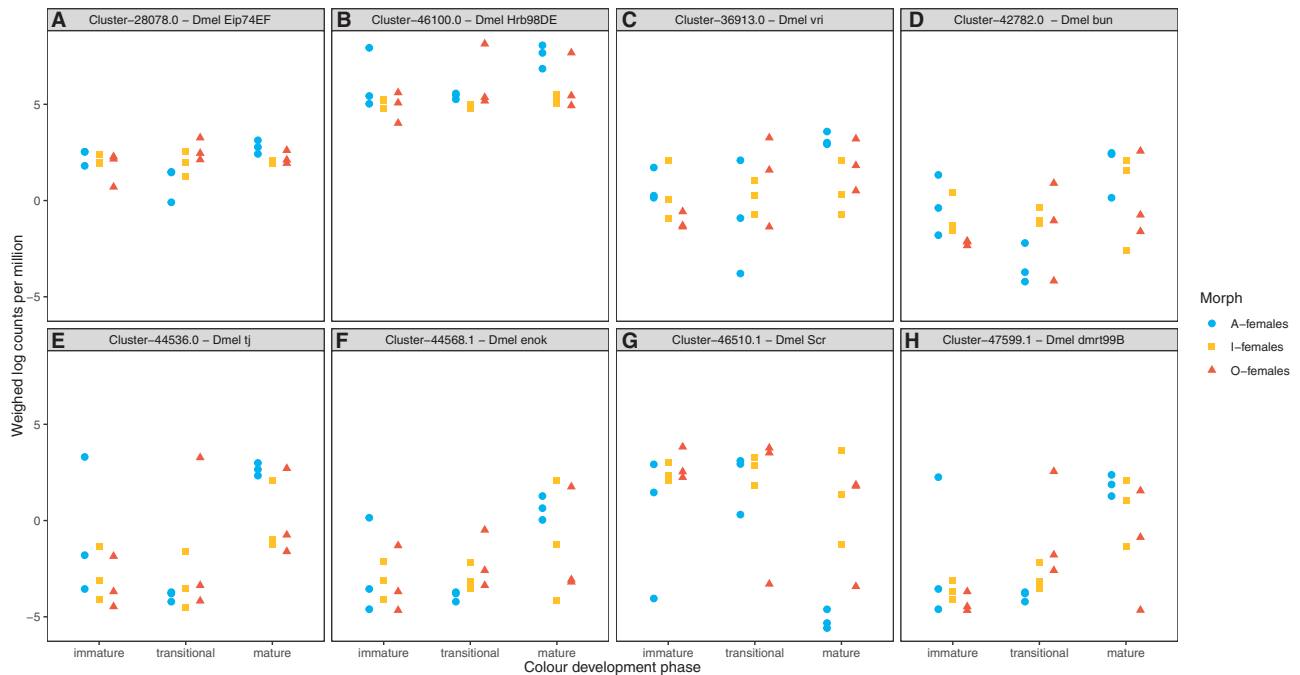
Table 3. Regulatory genes with different changes in gene expression between A- and both I- and O-female morphs in *I. elegans*, during *late* color development. CORSET clusters are assumed to represent *I. elegans* genes. Transcript sequences in these clusters were blasted against annotated proteins in the *Drosophila melanogaster* (Dmel) genome. For each of the queried *I. elegans* sequences, we report the best Dmel hit, its corresponding gene name, e-value, and inferred mode of regulation and function.

Cluster ID	Best Dmel hit	Gene name	e-value	Mode of regulation	Function	References
16360.1	Transcription termination factor, mitochondrial	*mTTF*	4.81×10^{-32}	Transcription factor	Regulates mitochondrial replication and transcription by interacting physically with helicase and polymerase enzymes	Roberti et al. (2005)
18749.0	T-related protein	brachyenteron	2.09×10^{-49}	Transcription factor	Fate determination of hindgut stem cells	Fox and Spradling (2009)
19883.1	Histone deacetylase complex subunit SAP30 homolog	*Sap30*	2.71×10^{-58}	Post-translational modification	Part of a corepressor complex that regulates G2/M cell cycle progression	Laherty et al. (1998)
28078.0	Ecdysone-induced protein E74	*Eip74EF*	1.01×10^{-52}	Transcription factor	Promotes germline proliferation and maintenance in ovaries	Ables and Drummond-Barbosa (2010)
31494.0	Enhancer of split mbeta protein	*E(spl)mbeta-HLH*	7.48×10^{-20}	Transcription factor	Repression of neural cell fate in response to Notch signaling	Jennings et al. (1994)
36913.0	Vrille	*vri*	7.43×10^{-46}	Transcription factor	Control of circadian rhythm, cardiac aging, ecdysone target in the ovary, associated with follicle cell maintenance and proliferation	Cyran et al. (2003); Monnier et al. (2012); Ables et al. (2016)
41360.2	Chromodomain-helicase-DNA-binding protein Mi-2 homolog	*Mi-2*	~0	Chromatin remodeling	Pro-neural gene repression	Yamasaki and Nishida (2006)
42782.0	Bunched	*bun*	6.00×10^{-31}	Transcription factor	Ovarian follicle cell development and migration, eggshell formation, neurblast proliferation, mushroom body development	Dobens et al. (1997); Dobens et al. (2000); Kim et al. (2009)

(Continued)

Table 3. Continued.

Cluster ID	Best Dmel hit	Gene name	e-value	Mode of regulation	Function	References
44536.0	Traffic jam	*tj*	2.66×10^{-29}	Transcription factor	Ovarian follicle cell migration, maintenance of ovarian stem cells	Gunawan et al. (2013); Panchal et al. (2017)
44568.1	Histone acetyltransferase	*enok*	8.66×10^{-110}	Post-translational modification	Neuroblast proliferation, maintenance of ovarian germ cells	Scott et al. (2001); Xin et al. (2013)
46100.0	Heterogeneous nuclear ribonucleoprotein A1	*Hrb98DE*	2.93×10^{-36}	mRNA splicing and export	maintenance and differentiation of ovarian germ cells,	He and Smith (2009); Ji and Tulin (2012)
46510.1	Homeotic protein Sex combs reduced	*Scr*	3.80×10^{-46}	Transcription factor	Induces and responds to the expression of *dsx* during sexual differentiation of somatic tissues	Barmina and Kopp (2007); Tanaka et al. (2011)
47599.1	Doublesex-Mab related 99B	*dmrt99B*	5.82×10^{-20}	Transcription factor	Integrates sex-determining, patterning and hormonal signals during somatic sexual differentiation	Kopp (2012)

Figure 6. Regulatory genes with different changes in gene expression between A- and both I- and O-females, during *late* color development of *I. elegans*. The symbols indicate expression levels of genes with inferred roles in regulating reproductive development (A–F) and sexual differentiation (G–H) in *D. melanogaster*. Expression data (log counts per million) have been weighed by within-sample variability and by the mean-variance relationship among genes, using "voom" (see Methods). Best hits in the *D. melanogaster* (Dmel) genome and inferred modes of regulation and functions are shown in Table 3.

revealed 18 genes (Table 3), most of which (∼89%) increased in expression in A-females, while remaining relatively constant or decreasing in I- and O-females. We again used *blastx* against the *D. melanogaster* genome to examine the potential functions of these regulatory genes. We focus on the 13 genes that had good hits (e-value $< 10 \times 10^{-5}$) against annotated proteins in SwissProt/TrEMBL (UniProt Consortium 2019). These genes comprised several transcription factors, including E74, a ribonucleoprotein and two proteins involved in histone acetylation (Table 3; Fig. 6). None of these regulatory genes varied significantly in expression patterns between I- and O-females, during either *early* or *late* color development.

Discussion

The genomic signatures and consequences of sexual antagonism and various forms of sexual conflict are gaining increased interest (Rowe et al. 2018), but with a few recent exceptions from studies on fruit flies, humans and flycatchers, empirical data in this area are limited (Barson et al. 2015; Cheng and Kirkpatrick 2016; Dutoit et al. 2018). We suggest that research in this area would benefit from gene expression studies on organisms with discrete genetic morphs, including female-limited polymorphisms, which are many times associated with sexual conflict between males

and females (Svensson et al. 2005; 2009; Reinhardt et al. 2007; Karlsson et al. 2013; Iversen et al. 2019). Here, we presented data on how different female morphs of the damselfly *I. elegans* change their gene expression profiles in different ways during the course of color development, as the morphs become sexually mature (Willink et al. 2019). One of the female morphs develops a male-like coloration at maturity, whereas the other two morphs develop color patterns strikingly different from that of males (Fig. 1B; Svensson et al. 2009). Morph differences in the direction, magnitude, or timing of gene expression changes during this developmental period could suggest direct or indirect interactions between the color-morph locus and loci underlying the multitude of phenotypic traits that differentiate the adult female morphs (Svensson and Abbott 2005; Lancaster et al. 2017; Willink and Svensson 2017; Willink et al. 2019; Svensson et al. 2020). Elucidating these interactions is important for a better understanding of the mechanisms behind pleiotropy of major-effect loci, and how these loci can produce phenotypically divergent and co-adapted morphs in damselflies and other insects.

In this study, we found that during the *early* phase of color development, between the *immature* and *transitional* phases, thousands of genes, controlling multiple metabolic processes, decreased in expression in all three female morphs (Tables 1 and S4; Fig. 2A). Widespread downregulation of gene expression

may indicate a shared slowdown in basic metabolism across all three morphs, which characterizes adult development in insects once energetically expensive tissues, such as gametes and flight muscle, have developed (Hack 1997; Piiroinen et al. 2010; Niitepõld and Hanski 2013). Conversely, most differences in gene expression changes among morphs were observed *late* in color development, between the *transitional* and *mature* developmental color phases (Fig. 4). During *late* color development, trajectories of gene expression changes diverged markedly between the male-mimicking A-females and both I- and O-females (Fig. 4B). I- and O-females also exhibited greater differentiation in developmental regulation of gene expression during *late* color development, but neither morph was as differentiated from the other two as A-females were (Fig. 4B). Moreover, the overall expression patterns of DE genes in I- and O-females remained positively correlated, in *late* as in *early* color development (Fig. 2A).

The male-mimicking A-females of *I. elegans* develop their final color pattern at an earlier age than the other two female morphs (Svensson et al. 2020; Figs. 1B and S1). Thus, one possible explanation for the distinctive gene expression profiles in A-females is that they accelerate color changes relative to other developmental processes, including sexual maturation. If so, A-females would become differentiated from I- and O-females during *late* color development primarily because of their younger age. Our results suggested that color development in A-females is indeed accelerated with respect to some other developmental processes, but not necessarily sexual maturation. DE genes across *early* and *late* color transitions were positively correlated in A-females only (Fig. 2B), as expected by the fact that the two color transitions occur over a shorter time period in this morph. However, this correlation was not particularly extreme, when compared to a random sample of genes (Fig. 2B). *Mature*-color A-females showed a somewhat increased tendency to exhibit reproductive failure compared to *mature*-color I-females, as expected if a larger proportion of *mature*-color A-females was still sexually immature. However, this difference was relatively small (less than 2% on average; Fig. 3), and it is therefore unlikely to account for the large differences in fecundity between A- and I-females in the field (Willink and Svensson 2017; Willink et al. 2019). Taken together with our recent previous work, these results suggest that heterochrony of color development relative to other developmental processes may explain some of the differences in fecundity and gene expression between A- and I-females. Yet, sexual maturation is also accelerated in A-females. In fact, these male-mimicking females achieved a relatively high rate of reproductive success after only two thirds of the color-development period of I- and O-females (Figs. 1B and 3). The reduced fecundity of the male-mimicking A-females might therefore be a pleiotropic cost caused by heterochrony, that this morph pays for its accelerated color development. However, the

results in the present study do not permit us to pinpoint the specific physiological or molecular mechanisms behind such a cost. The accelerated reproductive development in A-females might, however, be advantageous, especially at northern latitudes where mating seasons are cooler and shorter (Svensson et al. 2020).

Some previous studies on vertebrates suggest that a single locus or a tightly linked group of color-morph loci can influence reproductive physiology via hormonal regulation (Sinervo and Calsbeek 2003; Lamichhaney et al. 2016). In *I. elegans*, the color-morph locus might also interact via hormonal regulation with numerous other genes that influence egg development. We found that three *I. elegans* genes with inferred roles in the ecdysone biosynthesis pathway underwent changes in expression during *late* color development that were more pronounced (i.e., either more negative or more positive) in A-females than in the other two female morphs. One of these genes was inferred to code for 20EMO, the enzyme that catalyzes the conversion of E to 20E in the ovarian follicle and nurse cells of *D. melanogaster* (Table 2; Fig. 5C; Petryk et al. 2003). In insects, 20E induces ovarian cell development and is required in follicle cell differentiation and vitellogenesis (Swevers and Iatrou 2003; Simonet et al. 2004). In A-females of *I. elegans*, this putative gene increased in expression between the *transitional* and *mature* color phases, reaching an expression level similar to that of sexually mature I- and O-females, which are older on average (Figs. 1B and 5C). The two other genes with unique developmental changes in expression in A-females code for enzymes associated with upstream points in the ecdysone biosynthesis pathway (Table 2; Figs. 5A and 5B). Finally, an ecdysone responsive gene essential for oogenesis (E74) also showed increased expression during *late* color development in only A-females (Table 3; Fig. 6A). In *D. melanogaster*, E74 responds to ecdysone titers to promote germline proliferation during early oogenesis, and is key for preventing germline degeneration during later stages of oogenesis (Ables and Drummond-Barbosa 2010).

Our finding that both ecdysone biosynthesis genes and ecdysone-responsive genes changed in expression during the *late* color development of only A-females (Figs. 5 and 6A) suggests that the color morph locus might have pleiotropic effects via ecdysone signaling, regulating the timing of female reproductive development. This interpretation is also supported by the expression pattern of several other regulatory genes that are presumably involved in reproductive development (Table 3), all of which increased in expression between the *transitional* and *mature* color phases of only A-females (Fig. 6B–F). For instance, in *D. melanogaster*, a heterogeneous ribonucleoprotein (hnRNP) induces the expression of cadherin, which is in turn essential to maintain cell-cell adhesion during germline stem cell proliferation (Ji and Tulin 2012). hnRNPs can be responsive to ecdysone levels through association with the protein on ecdysone puffs

(Amero et al. 1993). In *I. elegans*, both hnRNP and cadherin genes increased in expression during the *late* color development of adult A-females (Figs. 6B and S4). In fact, *mature* color A-females had a higher expression level of this putative hnRNP gene than either I- or O-females (Fig. 6B). Also consistent with the accelerated sexual maturation in A-females, the set of genes that increased in expression during *late* color development in this morph was significantly enriched for multiple processes necessary for cell cycle progression, including meiotic cell cycle and division (Table S7). This was not the case for I- and O-females during the course of either *early* or *late* color development.

The regulatory genes that were differentially expressed in the male-mimicking A-females during *late* color development also suggest a role of the color-morph locus in inducing morph differentiation in somatic tissues of *I. elegans*. One of these genes mapped to *Dmrt* (Table 3), which is a gene family involved in sex determination and differentiation across animal taxa (Kopp 2012). This *Dmrt* gene underwent a greater increase in expression between the *transitional* and *mature* color phases in A-females compared to both I- and O-females. In somatic tissues of *D. melanogaster* another *Dmrt* gene, *doublesex* (*dsx*) integrates sexual identity, patterning, and hormonal signals to induce the development of sexually dimorphic structures (Kopp 2012). Alternative splicing of *dsx* also underpins the development of male-mimicry in the female polymorphic butterfly *Papilio polytes* (Kunte et al. 2014). In the *I. elegans* congener *I. senegalensis*, nonmimicking females are distinguished from both A-females and males in the expression pattern of a *dsx* isoform (Takahashi et al. 2018). *dsx* is therefore also a plausible regulator of the development of male mimicry in *I. elegans*, as it is differentially expressed between adult males and females (Chauhan et al. unpubl. ms.). However, we found no evidence of differential expression of the *Dmrt* gene *dsx* in *I. elegans* females, during the period of developmental color changes (Fig. S5A). The *Dmrt* gene differentially expressed during *late* color development in *I. elegans* lacks homology to the dimerization domain that characterizes *dsx* (Bayrer et al. 2005), but as all other *Dmrt* genes it contains a DM DNA binding motif, which confers regulatory capacity over pseudopalindromic DNA targets (Zhu et al. 2000).

Holometabolous insects have multiple *Dmrt* genes (Wexler et al. 2014), and *I. elegans* has at least two (Figs. 6H and S5A). However, the functions of the *Dmrt* genes other than *dsx* are poorly known in insects, although these genes might also integrate sexual identity and spatial and temporal signals during sexual differentiation (Picard et al. 2015). Although sex determination mechanisms are diverse across animal taxa, their downstream actions that result in sexual differentiation are typically more conserved and often rely on transcriptional regulation by the DM domain DNA binding motif (Zhu et al. 2000). In line with the possibility that this *Dmrt* gene may

contribute to the somatic differentiation of male-mimicking females in *I. elegans*, we found that genes that interact with *dsx* during the development of sexually dimorphic structures in *D. melanogaster* also had more drastic changes in expression during *late* color development in A-females than in either I- and O-females (Table 3; Figs. 6G and S5B–D).

This study of the developmental trajectories of color and gene expression changes in the female morphs of *I. elegans* contributes to understanding the mechanisms for pleiotropy of large-effect loci, such as those underpinning animal color polymorphisms. Our results suggest that the color-morph locus in *I. elegans* induces heterochrony in the male-mimicking A-females. These A-females show accelerated color changes and faster sexual maturation, the latter presumably caused by ecdysone signaling. We also uncovered hundreds of developmental changes in gene expression profiles that differed in direction or magnitude between A-females and both I- and O-females (Fig. 4B). There are three possible explanations for this pattern. First, some differences in gene expression changes during late color development may arise if *mature*-color A-females were younger than the other *mature*-color morphs. This could explain phenotypic differences in traits other than color and fecundity, both of which develop faster in A-females. Second, developmental genes with many downstream targets, such as *Dmrt* and homeotic genes (Table 3; Figs. 6G and 6H), may mediate unique expression changes of A-females through complex networks of gene-gene interactions. Third, the color locus may cause ecological differentiation between morphs via fewer direct interactions between genes, but with morph-specific micro-habitat selection, differential parasite loads, or differential intersexual interactions feeding back into the developmental regulation of gene expression. The latter two possibilities represent functional epistasis, whereby the phenotypic effects of genes or gene substitutions depend on the genetic background (Hansen and Wagner 2001), in this case, on the genotype at the color-morph locus. Theory shows that functional epistasis can play crucial roles in evolution by natural selection (e.g., Kimura and Maruyama 1966; Barton 1995; Rice 1998; Hansen 2013; Jones et al. 2014). However, to gauge its empirical importance, we need to better understand the dynamics of gene interactions over the course of development (Csilléry et al. 2018).

Conclusions

Female morphs of the common bluetail damselfly differ in their developmental trajectories of color change, sexual maturation, and changes in gene expression. Specifically, the male-mimicking A-female morph exhibits accelerated color and reproductive development, and becomes increasingly different from the two other female morphs in the pattern of developmental changes in gene expression, soon before the completion of

color development. Our results suggest that ecdysone signaling mediates epistatic interactions between the color-morph locus and genes influencing the development of female fecundity. Our results also point to other regulatory differences during this critical period of color development, such as a drastically increased expression of a *Dmrt* gene during the development of male-mimicking females. This study provides insights on how pronounced phenotypic differences between female morphs emerge during the course of development, and suggests that heterochrony and epistasis may underlie such pleiotropic effects of color morph loci in *I. elegans*. These results add to a growing understanding of how the evolution of regulatory architecture is shaped by sexual conflict.

AUTHOR CONTRIBUTIONS

EIS conceived the study with input from MCD and BW. MCD and BW obtained the sequence data. CW assembled the transcriptome. BW performed the differential expression analyses and functional annotations with help from MCD. BW wrote the manuscript with input from all authors.

ACKNOWLEDGMENTS

DATA ARCHIVING

Data are archived in Dryad (https://doi.org/10.5061/dryad.g1jwstqnd) and NCBI's Sequence Read Archive (BioProject #PRJNA624641).

LITERATURE CITED

Ables, E. T., and D. Drummond-Barbosa. 2010. The steroid hormone ecdysone functions with intrinsic chromatin remodeling factors to control female germline stem cells in *Drosophila*. Cell Stem Cell 7:581–592.

Ables, E. T., G. H. Hwang, D. S. Finger, T. D. Hinnant, and D. Drummond-Barbosa. 2016. A genetic mosaic screen reveals ecdysone-responsive genes regulating *Drosophila* oogenesis. G3-Genes Genom. Genet. 6:2629–2642.

Albertson, R. C., Y. L. Yan, T. A. Titus, E. Pisano, M. Vacchi, P. C. Yelick, H. W. Detrich, and J. H. Postlethwait. 2010. Molecular pedomorphism underlies craniofacial skeletal evolution in Antarctic notothenioid fishes. BMC Evol. Biol. 10:4.

Alexa, A., and J. Rahnenfuhrer. 2016. topGO: enrichment analysis for gene ontology. R package version 2.30.1. Available at: https://bioconductor.org/packages/release/bioc/html/topGO.html.

Alexa, A., J. Rahnenführer, and T. Lengauer. 2006. Improved scoring of functional groups from gene expression data by decorrelating GO graph structure. Bioinformatics 22:1600–1607.

Amero, S. A., M. J. Matunis, E. Matunis, J. W. Hockensmith, G. Raychaudhuri, and A. L. Beyer. 1993. A unique ribonucleoprotein complex assembles preferentially on ecdysone-responsive sites in *Drosophila melanogaster*. Mol. Cell. Biol. 13:5323–5330.

Andrade, P., C. Pinho, G. P. i de Lanuza, S. Afonso, J. Brejcha, C. J. Rubin, O. Wallerman, P. Pereira, S. J. Sabatino, A. Bellati, et al. 2019. Regulatory changes in pterin and carotenoid genes underlie balanced color polymorphisms in the wall lizard. Proc. Natl. Acad. Sci. USA 116:5633–5642.

Barmina, O., and A. Kopp. 2007. Sex-specific expression of a HOX gene associated with rapid morphological evolution. Dev. Biol. 311:277–286.

Barson, N. J., T. Aykanat, K. Hindar, M. Baranski, G. H. Bolstad, P. Fiske, C. Jacq, A. J. Jensen, S. E. Johnston, S. Karlsson, et al. 2015. Sex-dependent dominance at a single locus maintains variation in age at maturity in salmon. Nature 528:405–408.

Barton, N. H. 1995. A general model for the evolution of recombination. Genet. Res. 65:123–144.

Bayrer, J. R., W. Zhang, and M. A. Weiss. 2005. Dimerization of *Doublesex* is mediated by a cryptic ubiquitin-associated domain fold: implications for sex-specific gene regulation. J. Biol. Chem. 280:32989–32996.

Benjamini, Y., and Y. Hochberg. 1995. Controlling the false discovery rate: a practical and powerful approach to multiple testing. J. Royal Stat. Soc. 57:289–300.

Bolger, A. M., M. Lohse, and B. Usadel. 2014. Trimmomatic: a flexible trimmer for Illumina sequence data. Bioinformatics 30:2114–2120.

Camacho, C., G. Coulouris, V. Avagyan, N. Ma, J. Papadopoulos, K. Bealer, and T. L. Madden. 2009. BLAST+: architecture and applications. BMC Bioinf. 10:421.

Cheng, C., and M. Kirkpatrick. 2016. Sex-specific selection and sex-biased gene expression in humans and flies. PLoS Genet. 12:e1006170.

Conesa, A., S. Götz, J. M. Garcia-Gómez, J. Terol, M. Talón, and M. Robles. 2005. Blast2GO: a universal tool for annotation, visualization and analysis in functional genomics research. Bioinformatics 21:3674–3676.

Cordero, A. 1990. The inheritance of female polymorphism in the damselfly *Ischnura graellsii* (Rambur) (Odonata: Coenagrionidae). Heredity 64:341–346.

Cordero, A., S. S. Carbone, and C. Utzeri. 1998. Mating opportunities and mating costs are reduced in androchrome female damselflies, *Ischnura elegans* (Odonata). Anim. Behav. 55:185–197.

Csilléry, K., A. Rodríguez-Verdugo, C. Rellstab and F. Guillaume. 2018. Detecting the genomic signal of polygenic adaptation and the role of epistasis in evolution. Mol. Ecol. 27:606–612.

Cyran, S. A., A. M. Buchsbaum, K. L. Reddy, M. C. Lin, N. R. J. Glossop, P. E. Hardin, M. W. Young, R. V. Storti, and J. Blau. 2003. *vrille*, *Pdp1*, and *dClock* form a second feedback loop in the *Drosophila* circadian clock. Cell 112:329–341.

Davidson, N. M., and A. Oshlack. 2014. Corset: enabling differential gene expression analysis for de novo assembled transcriptomes. Genome Biol. 15:410.

Dijkstra, P. D., S. M. Maguire, R. M. Harris, A. A. Rodriguez, R. S. DeAngelis, S. A. Flores, and H. A. Hofmann. 2017. The melanocortin system regulates body pigmentation and social behaviour in a colour polymorphic cichlid fish. Proc. R. Soc. B 284:20162838.

Dobens, L. L., T. Hsu, V. Twombly, W. M. Gelbart, L. A. Raftery, and F. C. Kafatos. 1997. The *Drosophila* bunched gene is a homologue of the growth factor stimulated mammalian TSC-22 sequence and is required during oogenesis. Mech. Dev. 65:197–208.

Dobens, L. L., J. S. Peterson, J. Treisman, and L. A. Raftery. 2000. *Drosophila* bunched integrates opposing DPP and EGF signals to set the operculum boundary. Development 127:745–754.

Dutoit, L., C. F. Mugal, P. Bolívar, M. Wang, K. Nadachowska-Brzyska, L. Smeds, H. P. Yazdi, L. Gustafsson, and H. Ellegren. 2018. Sex biased gene expression, sexual antagonism and levels of genetic diversity in the collared flycatcher (*Ficedula albicollis*) genome. Mol. Ecol. 27:3572–3581.

Fisher, R. A. 1930. The genetical theory of natural selection. Clarendon, Oxford, U.K.

Flatt, T., M. Tu, and M. Tatar. 2005. Hormonal pleiotropy and the juvenile hormone regulation of *Drosophila* development and life history. Bioessays 27:999–1010.

Fox, D. T., and A. C. Spradling. 2009. The *Drosophila* hindgut lacks constitutively active adult stem cells but proliferates in response to tissue damage. Cell Stem Cell 5:290–297.

Gangoso, L., R. Gutiérrez-López, J. Martinez-de la Puente, and J. Figuerola. 2016. Genetic colour polymorphism is associated with avian malarial infections. Biol. Lett. 12:20160839.

Gavrilets, S., and D. Waxman. 2002. Sympatric speciation by sexual conflict. Proc. Natl. Acad. Sci. USA 99:10533–10538.

Gerhart, J., and M. Kirschner. 2007. The theory of facilitated variation. Proc. Natl. Acad. Sci. USA 104:8582–8589.

Gering, E. J. 2017. Male-mimicking females increase male-male interactions, and decrease male survival and condition in a female-polymorphic damselfly. Evolution 71:1390–1396.

Gomez, C., E. M. Özbudak, J. Wunderlich, D. Baumann, J. Lewis, and O. Pourquié. 2008. Control of segment number in vertebrate embryos. Nature 454:335–339.

Gosden, T. P., and E. I. Svensson. 2009. Density-dependent male mating harassment, female resistance, and male mimicry. Am. Nat. 173:709–721.

Gould, S. J. 1977. Ontogeny and phylogeny. Harvard Univ. Press, Cambridge, MA.

Grabherr, M. G., B. J. Haas, M. Yassour, J. Z. Levin, D. A. Thompson, I. Amit, X. Adiconis, L. Fan, R. Raychowdhury, Q. Zeng, et al. 2011. Full-length transcriptome assembly from RNA-Seq data without a reference genome. Nat. Biotechnol. 29:644–652.

Gunawan, F., M. Arandjelovic, and D. Godt. 2013. The Maf factor Traffic jam both enables and inhibits collective cell migration in *Drosophila* oogenesis. Development 140:2808–2817.

Gunter, H. M., C. Koppermann, and A. Meyer. 2014. Revisiting de Beer's textbook example of heterochrony and jaw elongation in fish: calmodulin expression reflects heterochronic growth, and underlies morphological innovation in the jaws of belonoid fishes. EvoDevo 5:8.

Haas, B. J., A. Papanicolaou, M. Yassour, M. Grabherr, P. D. Blood, J. Bowden, M. B. Couger, D. Eccles, B. Li, M. Lieber, et al. 2013. De novo transcript sequence reconstruction from RNA-seq using the Trinity platform for reference generation and analysis. Nat. Protoc. 8:1494–1512.

Hack, M. A. 1997. The effects of mass and age on standard metabolic rate in house crickets. Physiol. Entomol. 22:325–331.

Hadfield, J. D. 2010. MCMC methods for multi-response generalized linear mixed models: the MCMCglmm R package. J. Stat. Softw. 33:1–22.

Hansen, T. F., and G. P. Wagner. 2001. Modeling genetic architecture: a multilinear theory of gene interaction. Theor. Popul. Biol. 59:61–86.

Hansen T. F. 2013. Why epistasis is important for selection and adaptation. Evolution 67: 3501 –3511. https://doi.org/10.1111/evo.12214.

He, Y., and R. Smith. 2009. Nuclear functions of heterogeneous nuclear ribonucleoproteins A/B. Cell. Mol. Life Sci. 66:1239–1256.

Hemani, G., K. Shakhbazov, H. Westra, T. Esko, A. K. Henders, A. F. McRae, J. Yang, G. Gibson, N. G. Martin, A. Metspalu, et al. 2014. Detection and replication of epistasis influencing transcription in humans. Nature 508:249–253.

Henze, M. J., O. Lind, B. D. Wilts, and A. Kelber. 2019. Pterin-pigmented nanospheres create the colours of the polymorphic damselfly *Ischnura elegans*. J. Royal Soc. Interface 16:20180785.

Hill, M. S., M. Reuter, and A. J. Stewart. 2019. Sexual antagonism drives the displacement of polymorphism across gene regulatory cascades. Proc. R. Soc. Lond. B Biol. Sci. 286:20190660.

Hill, W. G., M. E. Goddard, and P. M. Visscher. 2008. Data and theory point to mainly additive genetic variance for complex traits. PLos Genet. 4:e1000008.

Huang, W., S. Richards, M. A. Carbone, D. Zhu, R. R. H. Anholt, J. F. Ayroles, L. Duncan, K. W. Jordan, F. Lawrence, M. M. Magwire, et al. 2012. Epistasis dominates the genetic architecture of *Drosophila* quantitative traits. Proc. Natl. Acad. Sci. USA 109:15553–15559.

Ioannidis, P., F. A. Simao, R. M. Waterhouse, M. Manni, M. Seppey, H. M. Robertson, B. Misof, O. Niehuis, and E. M. Zdobnov. 2017. Genomic features of the damselfly *Calopteryx splendens* representing a sister clade to most insect orders. Genome Biol. Evol. 9:415–430.

Iversen, L.L., E. I. Svensson, S. T. Christensen, J. Bergsten, and K. Sand-Jensen. 2019. Sexual conflict and intrasexual polymorphism promote assortative mating and halt population differentiation. Proc. R. Soc. Lond. B Biol. Sci. 286:20190251.

Jennings, B., A. Preiss, C. Delidakis, and S. Bray. 1994. The Notch signalling pathway is required for Enhancer of split bHLH protein expression during neurogenesis in the *Drosophila* embryo. Development 120:3537–3548.

Ji, Y., and A. V. Tulin. 2012. Poly (ADP-ribose) controls DE-cadherin-dependent stem cell maintenance and oocyte localization. Nat. Commun. 3:760.

Jones, A.G., R. Bürger and S. J. Arnold. 2014. Epistasis and natural selection shape the mutational architecture of complex traits. Nat. Commun. 5:3709.

Joron, M., R. Papa, M. Beltrán, N. Chamberlain, J. Mavárez, S. Baxter, M. Abanto, E. Bermingham, S. J. Humphray, J. Rogers, et al. 2006. A conserved supergene locus controls colour pattern diversity in *Heliconius* butterflies. PLoS Biol. 4:e303.

Karlsson, G. K., A. Kovalev, E. I. Svensson, and S. N. Gorb. 2013. Male clasping ability, female polymorphism and sexual conflict: fine-scale elytral morphology as a sexually antagonistic adaptation in female diving beetles. J. R. Soc. Interface 10:20130409.

Kim, J., S. Lee, M. Hwang, S. Ko, C. Min, and J. Kim-Ha. 2009. Bunched specifically regulates α/β mushroom body neuronal cell proliferation during metamorphosis. Neuroscience 161:46–52.

Kimura, M. and T. Maruyama. 1966. The mutational load with epistatic gene interactions in fitness. Genetics, 54:1337–1351.

Kopp, A. 2012. Dmrt genes in the development and evolution of sexual dimorphism. Trends Genet. 28:175–184.

Kunte, K., W. Zhang, A. Tenger-Trolander, D. H. Palmer, A. Martin, R. D. Reed, S. P. Mullen, and M. R. Kronforst. 2014. Doublesex is a mimicry supergene. Nature 507:229–232.

Laherty, C. D., A. N. Billin, R. M. Lavinsky, G. S. Yochum, A. C. Bush, J.-M. Sun, T.-M. Mullen, J. R. Davie, D. W. Rose, C. K. Glass, et al. 1998. SAP30, a component of the mSin3 corepressor complex involved in N-CoR-mediated repression by specific transcription factors. Mol. Cell 2:33–42.

Lamichhaney, S., G. Fan, F. Widemo, U. Gunnarsson, D. S. Thalmann, M. P. Hoeppner, S. Kerje, U. Gustafson, C. Shi, H. Zhang, et al. 2016. Structural genomic changes underlie alternative reproductive strategies in the ruff (*Philomachus pugnax*). Nat. Genet. 48:84–88.

Lancaster, L. T., R. Y. Dudaniec, B. Hansson, and E. I. Svensson. 2017. Do group dynamics affect colour morph clines during a range shift? J. Evol. Biol. 30:728–737.

Law, C. W., Y. Chen, W. Shi, and G. K. Smyth. 2014. voom: precision weights unlock linear model analysis tools for RNA-seq read counts. Genome Biol. 15:R29.

Law, C. W., M. Alhamdoosh, S. Su, G. K. Smyth, and M. E. Ritchie. 2016. RNA-seq analysis is easy as 1-2-3 with *limma*, *Glimma* and *edgeR*. F1000Research 5:1408.

Le Rouzic, A., T. F. Hansen, T. P. Gosden, and E. I. Svensson. 2015. Evolutionary time-series analysis reveals the signature of frequency-dependent selection on a female mating polymorphism. Am. Nat. 185:E182–E196.

Lee, J., H. Kim, S. Yoo, and J. Yoo. 2019. Common cuckoo females may escape male sexual harassment by color polymorphism. Sci. Rep. 9:7515.

Li, W., and A. Godzik. 2006. Cd-hit: a fast program for clustering and comparing large sets of protein or nucleotide sequences. Bioinformatics 22:1658–1659.

Lindtke, D., K. Lucek, V. Soria-Carrasco, R. Villoutreix, T. E. Farkas, R. Riesch, S. R. Dennis, Z. Gompert, and P. Nosil. 2017. Long-term balancing selection on chromosomal variants associated with crypsis in a stick insect. Mol. Ecol. 26:6189–6205.

Linksvayer, T. A., and M. J. Wade. 2005. The evolutionary origin and elaboration of sociality in the aculeate Hymenoptera: maternal effects, sib-social effects, and heterochrony. Q. Rev. Biol. 80:317–336.

Liu, R., A. Z. Holik, S. Su, N. Jansz, K. Chen, H. S. Leong, M. E. Blewitt, M.-L. Asselin-Labat, G. K. Smyth, and M. E. Ritchie. 2015. Why weight? Modelling sample and observational level variability improves power in RNA-seq analyses. Nucleic Acids Res. 43:e97.

Mackay, T. F. C. 2014. Epistasis and quantitative traits: using model organisms to study gene–gene interactions. Nat. Rev. Genet. 15:22–33.

McCarthy, D. J., Y. Chen, and G. K. Smyth. 2012. Differential expression analysis of multifactor RNA-Seq experiments with respect to biological variation. Nucleic Acids Res. 40:4288–4297.

McKinnon, J. S., and M. E. R. Pierotti. 2010. Colour polymorphism and correlated characters: genetic mechanisms and evolution. Mol. Ecol. 19:5101–5125.

Monnier, V., M. Iché-Torres, M. Rera, V. Contremoulins, C. Guichard, N. Lalevée, H. Tricoire, and L. Perrin. 2012. dJun and Vri/dNFIL3 are major regulators of cardiac aging in *Drosophila*. PLoS Genet. 8:e1003081.

Monteiro, A., and O. Podlaha. 2009. Wings, horns, and butterfly eyespots: how do complex traits evolve?PLoS Biol. 7:e1000037.

Moon, R.M., and A. Kamath. 2019. Re-examining escape behaviour and habitat use as correlates of dorsal pattern variation in female brown anole lizards, *Anolis sagrei* (Squamata: Dactyloidae). Biol. J. Linn. Soc. 126:783–795.

Niitepõld, K., and I. Hanski. 2013. A long life in the fast lane: positive association between peak metabolic rate and lifespan in a butterfly. J. Exp. Biol. 216:1388–1397.

O'Neil, S. T., and S. J. Emrich. 2013. Assessing *De Novo* transcriptome assembly metrics for consistency and utility. BMC Genomics 14:465.

O'Neil, S. T., J. D. K. Dzurisin, R. D. Carmichael, N. F. Lobo, S. J. Emrich, and J. J. Hellmann. 2010. Population-level transcriptome sequencing of nonmodel organisms *Erynnis propertius* and *Papilio zelicaon*. BMC Genomics 11:310.

Ono, H., K. F. Rewitz, T. Shinoda, K. Itoyama, A. Petryk, R. Rybczynski, M. Jarcho, J. T. Warren, G. Marqués, M. J. Shimell, et al. 2006. *Spook* and *Spookier* code for stage-specific components of the ecdysone biosynthetic pathway in Diptera. Dev. Biol. 298:555–570.

Panchal, T., X. Chen, E. Alchits, Y. Oh, J. Poon, J. Kouptsova, F. A. Laski, and D. Godt. 2017. Specification and spatial arrangement of cells in the germline stem cell niche of the *Drosophila* ovary depend on the Maf transcription factor Traffic jam. PLoS Genet. 13:e1006790.

Petryk, A., J. T. Warren, G. Marqués, M. P. Jarcho, L. I. Gilbert, J. Kahler, J.-P. Parvy, Y. Li, C. Dauphin-Villemant, and M. B. O'Connor. 2003. *Shade* is the *Drosophila* P450 enzyme that mediates the hydroxylation of ecdysone to the steroid insect molting hormone 20-hydroxyecdysone. Proc. Natl. Acad. Sci. USA 100:13773–13778.

Pham, T., S. M. Day, W. J. Glassford, T. M. Williams, and M. Rebeiz. 2017. The evolutionary origination of a novel expression pattern through an extreme heterochronic shift. Evol. Dev. 19:43–55.

Phipson, B., S. Lee, I. J. Majewski, W. S. Alexander, and G. K. Smyth. 2016. Robust hyperparameter estimation protects against hypervariable genes and improves power to detect differential expression. Ann. Appl. Stat. 10:946–963.

Picard, M. A. L., C. Cosseau, G. Mouahid, D. Duval, C. Grunau, È. Toulza, J.-F. Allienne, and J. Boissier. 2015. The roles of *Dmrt* (Double sex/Male-abnormal-3 Related Transcription factor) genes in sex determination and differentiation mechanisms: Ubiquity and diversity across the animal kingdom. C. R. Biol. 338:451–462.

Piiroinen, S., L. Lindström, and A. Lyytinen. 2010. Resting metabolic rate can vary with age independently from body mass changes in the Colorado potato beetle, *Leptinotarsa decemlineata*. J. Insect Physiol. 56:277–282.

R Core Team. 2020. R: a language and environment for statistical computing. R Foundation for Statistical Computing, Vienna, Austria.

Reinhardt, K., E. Harney, R. Naylor, S. Gorb, and M. T. Siva-Jothy. 2007. Female-limited polymorphism in the copulatory organ of a traumatically inseminating insect. Am. Nat. 170:931–935.

Rice, S.H. 1998. The evolution of canalization and the breaking of von Baer's laws: modeling the evolution of development with epistasis. Evolution 52:647–656.

Ritchie, M. E., B. Phipson, D. Wu, Y. Hu, C. W. Law, W. Shi, and G. K. Smyth. 2015. *limma* powers differential expression analyses for RNA-sequencing and microarray studies. Nucleic Acids Res. 43:e47.

Roberti, M., P. Fernandez-Silva, P. L. Polosa, E. Fernandez-Vizarra, F. Bruni, S. Deceglie, J. Montoya, M. N. Gadaleta, and P. Cantatore. 2005. In vitro transcription termination activity of the *Drosophila* mitochondrial DNA-binding protein DmTTF. Biochem. Biophys. Res. Commun. 331:357–362.

Robinson, M. D., and A. Oshlack. 2010. A scaling normalization method for differential expression analysis of RNA-seq data. Genome Biol. 11:R25.

Robinson, M. D., D. J. McCarthy, and G. K. Smyth. 2010. *edgeR*: a bioconductor package for differential expression analysis of digital gene expression data. Bioinformatics 26:139–140.

Rowe, L., S. F. Chenoweth, and A. F. Agrawal. 2018. The genomics of sexual conflict. Am. Nat. 192:274–286.

Sánchez-Guillén, R. A., H. Van Gossum, and A. Cordero Rivera. 2005. Hybridization and the inheritance of female color polymorphism in two ischnurid damselflies (Odonata: Coenagrionidae). Biol. J. Linn. Soc. 85:471–481.

Schindelin, J., I. Arganda-Carreras, E. Frise, V. Kaynig, M. Longair, T. Pietzsch, S. Preibisch, C. Rueden, S. Saalfeld, B. Schmid, et al. 2012. Fiji: an open-source platform for biological-image analysis. Nat. Methods 9:676–682.

Scott, E. K., T. Lee, and L. Luo. 2001. *enok* encodes a *Drosophila* putative histone acetyltransferase required for mushroom body neuroblast proliferation. Curr. Biol. 11:99–104.

Shao, H., L. C. Burrage, D. S. Sinasac, A. E. Hill, S. R. Ernest, W. O'Brien, H. Courtland, K. J. Jepsen, A. Kirby, E. J. Kulbokas, et al. 2008. Genetic architecture of complex traits: large phenotypic effects and pervasive epistasis. Proc. Natl. Acad. Sci. USA 105:19910–19914.

Simonet, G., J. Poels, I. Claeys, T. Van Loy, V. Franssens, A. De Loof, and J. V. Broeck. 2004. Neuroendocrinological and molecular aspects of insect reproduction. J. Neuroendocrinol. 16:649–659.

Sinervo, B., and R. Calsbeek. 2003. Physiological epistasis, ontogenetic conflict and natural selection on physiology and life history. Integr. Comp. Biol. 43:419–430.

Smyth, G. K. 2004. Linear models and empirical bayes methods for assessing differential expression in microarray experiments. Stat. Appl. Genet. Mol. Biol. 3:1–25.

Smyth, G. K., M. Ritchie, N. Thorne, J. Wettenhall, W. Shi, and Y. Hu. 2018. limma: linear models for microarray and RNA-Seq data user's guide. Available via http://bioconductor.org/packages/release/bioc/html/limma.html.

Suzek, B. E., Y. Wang, H. Huang, P. B. McGarvey, C. H. Wu, and U. Consortium. 2014. UniRef clusters: a comprehensive and scalable alternative for improving sequence similarity searches. Bioinformatics 31:926–932.

Svensson, E. I. 2017. Back to basics: using colour polymorphisms to study evolutionary processes. Mol. Ecol. 26:2204–2211.

Svensson, E. I., and J. Abbott. 2005. Evolutionary dynamics and population biology of a polymorphic insect. J. Evol. Biol. 18:1503–1514.

Svensson, E. I., J. Abbott, and R. Härdling. 2005. Female polymorphism, frequency dependence, and rapid evolutionary dynamics in natural populations. Am. Nat. 165:567–576.

Svensson, E. I., J. K. Abbott, T. P. Gosden, and A. Coreau. 2009. Female polymorphisms, sexual conflict and limits to speciation processes in animals. Evol. Ecol. 23:93.

Svensson, E. I., B. Willink, M. C. Duryea, and L. T. Lancaster. 2020. Temperature drives pre-reproductive selection and shapes the biogeography of a female polymorphism. Ecol. Lett. 23:149–159.

Swevers, L., and K. Iatrou. 2003. The ecdysone regulatory cascade and ovarian development in lepidopteran insects: insights from the silkmoth paradigm. Insect Biochem. Mol. Biol. 33:1285–1297.

Takahashi, Y., J. Yoshimura, S. Morita, and M. Watanabe. 2010. Negative frequency dependent selection in female color polymorphism of a damselfly. Evolution 64:3620–3628.

Takahashi, M., Y. Takahashi, and M. Kawata. 2018. Candidate genes associated with color morphs of female-limited polymorphisms of the damselfly *Ischnura senegalensis*. Heredity 122:81–92.

Tanaka, K., O. Barmina, L. E. Sanders, M. N. Arbeitman, and A. Kopp. 2011. Evolution of sex-specific traits through changes in HOX-dependent doublesex expression. PLoS Biol. 9:e1001131.

Thomas, J. A., J. W. H. Trueman, A. Rambaut, and J. J. Welch. 2013. Relaxed phylogenetics and the Palaeoptera problem: resolving deep ancestral splits in the insect phylogeny. Syst. Biol. 62:285–297.

Thurmond, J., J. L. Goodman, V. B. Strelets, H. Attrill, L. S. Gramates, S. J. Marygold, B. B. Matthews, G. Millburn, G. Antonazzo, V. Trovisco, et al. 2019. FlyBase 2.0: the next generation. Nucleic Acids Res. 47:D759–D765.

Timmermans, M. J. T. N., S. W. Baxter, R. Clark, D. G. Heckel, H. Vogel, S. Collins, A. Papanicolaou, I. Fukova, M. Joron, M. J. Thompson, et al. 2014. Comparative genomics of the mimicry switch in *Papilio dardanus*. Proc. R. Soc. Lond. B Biol. Sci. 281:20140465.

Toomey, M. B., C. I. Marques, P. Andrade, P. M. Araújo, S. Sabatino, M. A. Gazda, S. Afonso, R. J. Lopes, J. C. Corbo, and M. Carneiro. 2018. A non-coding region near Follistatin controls head colour polymorphism in the Gouldian finch. Proc. R. Soc. Lond. B Biol. Sci. 285:20181788.

Tyler, A. L., F. W. Asselbergs, S. M. Williams, and J. H. Moore. 2009. Shadows of complexity: what biological networks reveal about epistasis and pleiotropy. Bioessays 31:220–227.

UniProt Consortium. 2019. UniProt: a worldwide hub of protein knowledge. Nucleic Acids Res. 47:D506–D515.

Vera, J. C., C. W. Wheat, H. W. Fescemyer, M. J. Frilander, D. L. Crawford, I. Hanski, and J. H. Marden. 2008. Rapid transcriptome characterization for a nonmodel organism using 454 pyrosequencing. Mol. Ecol. 17:1636–1647.

Waller, J. T., and E. I. Svensson. 2017. Body size evolution in an old insect order: no evidence for Cope's Rule in spite of fitness benefits of large size. Evolution 71:2178–2193.

West-Eberhard, M. J. 2003. Developmental plasticity and evolution. Oxford Univ. Press, New York.

Wexler, J. R., D. C. Plachetzki, and A. Kopp. 2014. Pan-metazoan phylogeny of the DMRT gene family: a framework for functional studies. Dev. Genes Evol. 224:175–181.

Willink, B., and E. I. Svensson. 2017. Intra-and intersexual differences in parasite resistance and female fitness tolerance in a polymorphic insect. Proc. R. Soc. Lond. B Biol. Sci. 284:20162407.

Willink, B., Duryea, M. C., & Svensson, E. I.2019. Macroevolutionary origin and adaptive function of a polymorphic female signal involved in sexual conflict. Am. Nat. 194:707–724.

Wood, A. R., M. A. Tuke, M. A. Nalls, D. G. Hernandez, S. Bandinelli, A. B. Singleton, D. Melzer, L. Ferrucci, T. M. Frayling, and M. N. Weedon. 2014. Another explanation for apparent epistasis. Nature 514:E3–E5.

Woronik, A., K. Tunström, M. W. Perry, R. Neethiraj, C. Stefanescu, M. de la Paz Celorio-Mancera, O. Brattström, J. Hill, P. Lehmann, R. Käkelä, and C. W. Wheat. 2019. A transposable element insertion is associated with an alternative life history strategy. Nat. Commun. 10:1–11.

Wright, S. 1930. The genetical theory of natural selection: a review. J. Hered. 21:349–356.

———. 1931. Evolution in Mendelian populations. Genetics 16:97–159.

Xin, T., T. Xuan, J. Tan, M. Li, G. Zhao, and M. Li. 2013. The *Drosophila* putative histone acetyltransferase Enok maintains female germline stem cells through regulating Bruno and the niche. Dev. Biol. 384:1–12.

Yamasaki, Y., and Y. Nishida. 2006. Mi-2 chromatin remodeling factor functions in sensory organ development through proneural gene repression in *Drosophila*. Dev. Growth Differ. 48:411–418.

Yassin, A., E. K. Delaney, A. J. Reddiex, T. D. Seher, H. Bastide, N. C. Appleton, J. B. Lack, J. R. David, S. F. Chenoweth, J. E. Pool, et al. 2016. The pdm3 locus is a hotspot for recurrent evolution of female-limited color dimorphism in *Drosophila*. Curr. Biol. 26:2412–2422.

Zhu, L., J. Wilken, N. B. Phillips, U. Narendra, G. Chan, S. M. Stratton, S. B. Kent, and M. A. Weiss. 2000. Sexual dimorphism in diverse metazoans is regulated by a novel class of intertwined zinc fingers. Genes Dev. 14:1750–1764.

Zinna, R., D. Emlen, L. C. Lavine, A. Johns, H. Gotoh, T. Niimi, and I. Dworkin. 2018. Sexual dimorphism and heightened conditional expression in a sexually selected weapon in the Asian rhinoceros beetle. Mol. Ecol. 27:5049–5072.

Associate Editor: S. Immler
Handling Editor: T. Chapman